CARBON 68 (2014) 369–379

Available at www.sciencedirect.com

ScienceDirect

journal homepage: www.elsevier.com/locate/carbon

The effect of temperature on the morphology and chemical surface properties of nitrogen-doped carbon nanotubes

Kambiz Chizari [a], *Alexander Vena* [a], *Lars Laurentius* [b], *Uttandaraman Sundararaj* [a,*]

[a] *Department of Chemical and Petroleum Engineering, University of Calgary, Calgary, Alberta, Canada*
[b] *Department of Chemistry, National Institute for Nanotechnology, University of Alberta, Edmonton, Alberta, Canada*

ARTICLE INFO

Article history:
Received 4 September 2013
Accepted 6 November 2013
Available online 15 November 2013

ABSTRACT

One of the most effective ways to tune the physical and chemical properties of CNTs is to dope them with a foreign element, such as nitrogen. Nitrogen atoms that are incorporated into the CNT structure can drastically change the properties of CNTs. The properties of nitrogen-doped carbon nanotubes (N-CNTs) originate from their structure; thus, it is practical to create a desired structure during synthesis. We have investigated the effects of synthesis parameters, mainly temperature, on various characterizations of N-CNTs, such as their morphologies, dimensions (diameter and length), defects, nitrogen inclusions and thermal stability. The results revealed strong correlations between the synthesis parameters and the properties of the synthesized N-CNTs. XPS characterization indicated that the percentage of nitrogen inclusion decreased with increasing synthesis temperature up to 850 °C and then increased at 950 °C. Raman spectroscopy showed a decrease in the number of defects in the N-CNT structure with increasing synthesis temperature. Finally TGA demonstrated a trend of increasing thermal stability of N-CNTs with increasing synthesis temperature, up to 850 °C then a reduced thermal stability at 950 °C. Based on these results, one can control the properties of N-CNTs and obtain materials with the desired characteristics by choosing the appropriate synthesis conditions.

1. Introduction

Since the discovery of carbon nanotubes (CNTs) in 1991 [1], there have been a huge number of research studies that have shown the unique properties of CNTs and their potential applications. One of the main keys to making the appropriate CNTs for a specific application is the ability to tune the physicochemical properties of CNTs via the modification of their structures. These structural modifications can be done by altering CNTs' diameters, lengths, number of defects in the structure, CNT wall thickness, and functionalizations.

One of the most efficient ways to change the properties of CNTs is through doping. Nitrogen and boron are the two most frequently used substitutions for carbon atoms in the structure of CNTs, due to the small differences in their atomic radii compared with that of carbon [2–5]. Introducing dopants can drastically change the physicochemical properties of CNTs, i.e., morphology, basicity, electrical and thermal conductivity [6–8]. A bamboo-shaped structure has been reported for nitrogen-doped carbon nanotubes (N-CNTs). The bamboo-shaped N-CNTs with channels closed by carbon arches have very different morphology than the undoped open-channel CNTs [7–9].

* *Corresponding author:* Fax: +1 403 284 4852.
E-mail address: u.sundararaj@ucalgary.ca (U. Sundararaj).
0008-6223/$ - see front matter
http://dx.doi.org/10.1016/j.carbon.2013.11.013

Different potential applications have been reported for N-CNTs in various fields, such as field emission devices [10,11], energy storage [12], gas sensors [4,13], composites [14] and catalysis [6,9,15,16]. One of the most outstanding potential applications found for N-CNTs is as a catalyst for oxygen reduction reactions (ORR) in fuel cells [6,17–22]. Gong et al. reported that N-CNTs can be an efficient candidate as a replacement for the expensive catalysts, such as platinum, used for ORR in fuel cells [6].

The physicochemical properties of N-CNTs depend on the type of incorporated nitrogen and the number of defects in the structure. There are at least three different types of nitrogen incorporations found in N-CNT structures: pyridinic, pyrrolic and quaternary nitrogen. Ghosh et al. [23] reported that the quaternary nitrogen substituents give rise to additional sub-levels in the unoccupied states near the Fermi level, while pyridinic nitrogen substituents destroy the existing sub-levels. These results show that the electrical properties can be modified by controlling the concentration of different types of nitrogen incorporation. Van Dommele et al. [15] reported an increase in catalytic activity of N-CNTs with higher concentrations of pyridinic nitrogen substituents for Knoevenagel condensation.

Various kinds of nitrogen sources have been used for N-CNT synthesis, i.e., nitrogen gas (N_2) [24], ammonia (NH_3) [25], pyridine [26], acetonitrile [27], melamine [28–30], dimethylformamide [31], 2-amino-4,6-dichloro-s-triazine ($C_3N_3C_{l2}$-NH_2) [32], nickel phthalocyanine ($NiC_{32}N_8H_{16}$) [33,34], iron phthalocyanine ($FeC_{32}N_8H_{16}$) [35] and benzylamine [36]. Ammonia is one of the most useful precursors of nitrogen in CNT doping [25,37–42] because ammonia is in a gaseous form at room temperature and can simply be added to the chemical vapor deposition (CVD) setup for CNT synthesis to obtain N-CNTs. The percentage of nitrogen doped in CNTs can be controlled by varying the ammonia flow rate and/or synthesis temperature [37,38]. Acetonitrile and pyridine are two other popular nitrogen precursors for the synthesis of N-CNTs [15,26,27,43,44]. However, the toxicity of these materials should be taken into account during the scale-up of the synthesis.

The percentage and type of nitrogen incorporation in the structure of N-CNTs depend on synthesis conditions, such as temperature and the type of nitrogen and carbon precursors. Synthesis of N-CNTs with high concentrations of nitrogen incorporated in the structure, i.e., a nitrogen-to-carbon ratio up to 20%, was reported using acetonitrile as the nitrogen source and CVD as the synthesis method [27]. Zhang et al. reported an increase in the percentage of nitrogen content in the structure of N-CNTs when increasing the synthesis temperature from 750 to 900 °C and a decrease in nitrogen content when increasing the temperature from 900 to 950 °C [45]. In another work, van Dommele et al. showed that the amount of nitrogen in the structure of N-CNTs had a mostly decreasing trend with increasing temperature [46]. These results show that the percentage of nitrogen content in N-CNTs can be varied by changing the synthesis temperature but its increasing or decreasing trend is not well known and needs more investigation.

The synthesis temperature not only affects the percentage of nitrogen doped in the N-CNT structure, but also influences the yield of the synthesis, the diameter of the N-CNTs, and the type of nitrogen incorporated into the N-CNTs [9,45,46]. Since the physicochemical properties of N-CNTs are dependent on the morphology of N-CNTs and the percentage and type of doped nitrogen, the control of these aspects is important [8,47,48]. Despite the importance of controlling the properties of N-CNTs, very few studies have been dedicated to the subject.

This article reports on the investigation of the effects of the synthesis temperature on the properties of nitrogen-doped carbon nanotubes. The synthesis of the N-CNTs was performed via a CVD method using alumina-supported iron as the catalyst. Different characterization methods, such as X-ray photoelectron spectroscopy (XPS), scanning electron microscopy (SEM), transmission electron microscopy (TEM), Raman spectroscopy and thermogravimetric analysis (TGA), were used for the determination of the morphology and physicochemical properties of N-CNTs.

2. Experimental

2.1. Catalyst preparation

Alumina-supported iron catalyst (Fe/Al_2O_3) was prepared by incipient wetness impregnation of iron nitrate (iron (III) nitrate nonahydrate, Baker Analyzed® ACS Grade) on an aluminum oxide support (Sasol Catalox SBa-200), followed by drying, calcination and reduction. The iron loading was set at 20 wt.%. The catalyst was dried at room temperature for 24 h and at 100 °C for 2 h. The calcination was done at 350 °C under air flow with a flow rate of 100 sccm for 4 h, in order to transform the iron nitrate precursor into its corresponding oxide. It was then ground and sieved to obtain a fine powder. The catalyst was further reduced in hydrogen (Praxair HY 5.0UH-T) flow with a flow rate of 100 sccm at 400 °C for 1 h, in order to obtain metallic iron supported on alumina.

2.2. Synthesis

The N-CNTs were synthesized via a CVD method using a mixture of ethane, ammonia and argon. Ethane (Praxair ET 2.0-K) was used as a source of carbon and ammonia (Praxair AM 4.5-K) as a source of nitrogen. The alumina-supported iron catalyst was placed inside a quartz boat located inside a quartz tubular reactor with an inner diameter of 4.5 cm. This reactor was placed inside a tube furnace (Thermo Scientific – Lindberg Blue M) with a thermocouple located in the middle of the hot zone at a distance of 2.5 cm to the reactor.

The differences between the temperature on the catalyst inside the reactor (sample temperature) and the temperature shown on the furnace controller (furnace temperature) were measured by an external thermocouple located on the catalyst powder inside the reactor at different temperatures, ranging from 400 to 950 °C under argon with a flow rate of 150 sccm. The sample temperature was 70 °C higher than the furnace temperature at 400 °C, and this difference decreased to 20 °C at 950 °C. The synthesis temperatures reported in this

article are the furnace temperatures. The flow rates of the gases were controlled by the gas flowmeters (Cole Parmer 150-mm 316 SS).

The synthesis temperature varied between 550 and 950 °C for different trials. The synthesis time, catalyst mass and gas total flow rate were kept constant at 2 h, 0.6 g and 150 sccm, respectively (Table 1). In order to investigate the influence of synthesis time on the yield and length of N-CNTs, different synthesis time ranging between 0.5 and 3 h were tested while keeping the synthesis temperature constant at 750 °C.

In order to compare some of the properties of N-CNTs to undoped carbon nanotubes, pristine CNTs were synthesized by replacing the ammonia gas (source of nitrogen) with hydrogen. Undoped CNTs were synthesized at two different temperatures (650 and 750 °C), and the other synthesis parameters were similar to the N-CNTs synthesis.

2.3. *Characterization techniques*

A Physical Electronics PHI VersaProbe 5000-XPS was used to record XPS spectra. The spectra were taken using a monochromatic aluminum source at 1486.6 eV and 49.3 W with a beam diameter of 200.0 μm. The samples were pressed on double-sided tape; and, a double neutralization, i.e., a low energy electron beam and low energy Ar^+ beam, were used during spectrum taking. The binding energies were reported relative to C1s at 284.8 eV.

For each sample, a high sensitivity mode spectrum was taken with a wide binding energy range of 0–1350 eV (survey) to determine the surface elemental composition of the samples. After determining which elements were present in the sample, a narrower binding energy window with a pass energy of 23.50 eV was used to get high energy resolution spectra of the elements present in the sample to determine its chemical environment and quantification.

The thermal resistivity of N-CNTs was tested using a Thermogravimetric Analyzer TGA (TA instruments – Q500). The samples were heated under air atmosphere (Praxair AI IND-K) from room temperature to 850 °C at a rate of 10 °C/min. The sample was held at 850 °C for 10 min before cooling.

The morphology of carbon nanotubes was observed with SEM and TEM. All TEM work was carried out on a Tecnai TF20 G2 FEG-TEM (FEI, Hillsboro, Oregon, USA) at 200 kV acceleration voltage with the standard single tilt holder. The images were captured on a Gatan UltraScan 4000 CCD (Gatan, Pleasanton, California, USA) at 2048 × 2048 pixels. The nanotubes were suspended in ethanol and sonicated for 5 min. A drop of this suspension was placed on one side of a standard TEM grid that was covered with a ~40 nm thin holey carbon film (EMS, Hatfield, Pennsylvania, USA) and left to dry for several minutes. The SEM work was carried on a Philips XL30 ESEM using 20 kV acceleration voltage. The SEM samples were prepared by spreading the carbon nanotubes powder on a conductive tape located on a SEM metallic sample holder. The sizes of CNTs were measured using MeasureIT software by created by Olympus Soft Imaging Solutions GmbH.

The structural defects of the N-CNTs were investigated using Raman spectroscopy. The powder samples of the N-CNTs were deposited on clean gold substrates and analyzed. The gold substrates were fabricated by coating a glass microscope slide with an adhesive layer of 5 nm of chromium followed by 300 nm of gold in a thermal evaporation system (Torr International). The Raman spectra were recorded with a Renishaw inVia Raman microscope. Radiation of 514 nm from an argon-ion laser was used for excitation. The Raman spectra for the N-CNTs were obtained by integrating the powder samples for 500 s with a laser power at the sample of 3.0 ± 0.2 mW. All spectra were collected with a 5× objective. The listed values for ratios comprised out of D-, G-, and G′-band intensities are averages based on intensity measurements obtained from baselined Raman spectra derived from a minimum of 3 different locations on the powder sample.

Table 1 – Synthesis conditions.

Parameter	Values
Synthesis temperature	550–950 °C
Synthesis time	2 h
Mass of catalyst	0.6 g
Wt.% of Fe on Al_2O_3	20%
Gas total flow rate	150 sccm
NH_3:C_2H_6:Ar flow rates	50:50:50 sccm

3. Results and discussion

3.1. *The effect of temperature on the properties of N-CNTs*

3.1.1. *Nitrogen incorporation*

The effects of the synthesis temperature on the nitrogen content in carbon nanotubes were investigated using XPS analysis. The atomic percentages of nitrogen compared to carbon (N/C at.%) as a function of the synthesis temperature are shown in Fig. 1. Increases in the synthesis temperature led to decreases in the concentration of nitrogen in the N-CNTs structure. This trend can be attributed to the higher number of defects and lower crystallinity of the N-CNTs synthesized at lower temperatures, which leads to easier acceptance of foreign elements into the structure.

Liu et al. related the decrease of N/C atomic percentage (at.%) with increasing synthesis temperature to the fact that the C—C bonding energy is higher than the C—N bonding energy; thus, the formation of the C—C bonding is expected to be more favorable than that of C—N [38]. At high temperatures, stable N_2 molecules can also be formed and leave the reaction zone without participating in the N-CNT structure. Bitter and his co-workers attributed this phenomenon to the easier formation of iron carbides compared to iron nitrides on the catalyst at higher temperatures, which leads to the lower participation of nitrogen in the N-CNT structure [46].

The results show that, in order to obtain a higher percentage of nitrogen doping in N-CNTs, lower synthesis temperatures should be used. The N-CNTs synthesized at 950 °C did not follow this trend, as the percentage of nitrogen increased to about 3 at.%. This may be related to the formation of other types of carbon allotropes, such as amorphous carbon, that can accept nitrogen easier in the structure. The presence of amorphous carbon in the N-CNTs synthesized at 950 °C is discussed further in Sections 3.1.2 and 3.1.4.

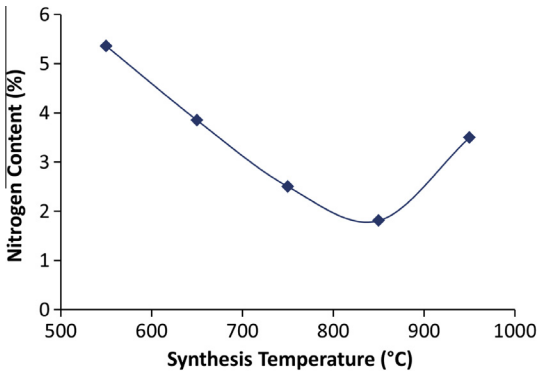

Fig. 1 – Nitrogen content in the structure of N-CNTs as a function of synthesis temperature. (A color version of this figure can be viewed online.)

The synthesis temperature not only affected the percentage of nitrogen incorporated in N-CNT structure, but it also varied the type of the nitrogen incorporation (N-types). There were at least four different N-types that could be found in the N-CNT structure. The N-types could be distinguished by the aid of XPS. XPS peaks could be assigned to the pyridinic nitrogen (398.3–399.8 eV), pyrrolic nitrogen (400.1–400.5 eV), quaternary nitrogen (401.0–401.4 eV) and to nitrogen oxide species and/or intercalated nitrogen molecules (404.0–405.6 eV) [9,49–52].

The XPS N1s spectra of the N-CNTs synthesized at different synthesis temperatures are shown in the Fig. 2A–E. According to the XPS results, the synthesis temperature played an important role on the type of nitrogen incorporation. The percentage of different N-types shown in Fig. 2F demonstrates that the quaternary nitrogen was more resistant to higher temperatures. Increasing the synthesis temperature decreased the overall percentage of nitrogen incorporated in the N-CNT structure, which can be mainly attributed to the loss of pyridinic and pyrrolic nitrogen. The decrease of the pyridinic nitrogen compared to quaternary nitrogen with increasing temperature using different types of catalysts and carbon and nitrogen sources has previously been reported [9,11,46].

3.1.2. *Morphology*

The morphology of the N-CNTs was investigated with SEM and TEM. SEM micrographs of N-CNTs are shown in the Fig. 3. The population density of the N-CNTs grown at the temperature of 550 °C was very low, indicating that this temperature was not sufficient for the effective growth of N-CNTs. By increasing the synthesis temperature to 750 °C, the length and population density of the N-CNTs increased considerably. At higher temperatures (850–950 °C), the N-CNTs population density was still high, but the diameter distribution was less homogeneous with a higher average diameter.

The average diameters of the N-CNTs were the mean values calculated using measurements of diameters of more than 70 N-CNTs per sample by using MeasureIT software. The results are shown in Fig. 4. The increase in N-CNT diameter can be attributed to the migration and sintering of the iron catalyst at high temperatures. These larger catalyst particles can lead to the formation of CNTs with larger diameters [53,54]. The smaller average diameter of N-CNTs at lower temperatures can be also related to the lower activity of large iron particles at low temperatures; therefore, the majority of the catalysts responsible for the growth of N-CNTs would be the particles with smaller sizes.

The TEM micrographs of N-CNTs revealed that the CNTs mainly had a bamboo-like structure, a characteristic that differs them from the usual open-channel undoped CNTs. The bamboo-like structure of N-CNTs has previously been re-

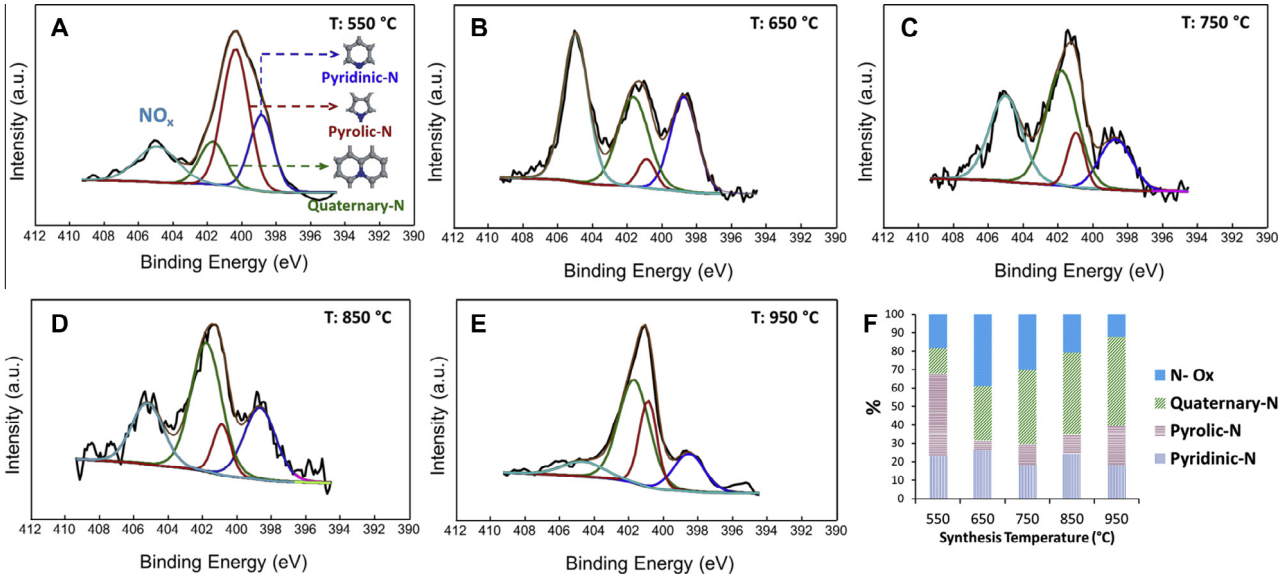

Fig. 2 – (A–E) XPS N1s spectra of the N-CNTs synthesized at different temperatures in the range between 550 and 950 °C. (F) The percentages of different N-types are plotted for the N-CNTs synthesized at different temperatures. (A color version of this figure can be viewed online.)

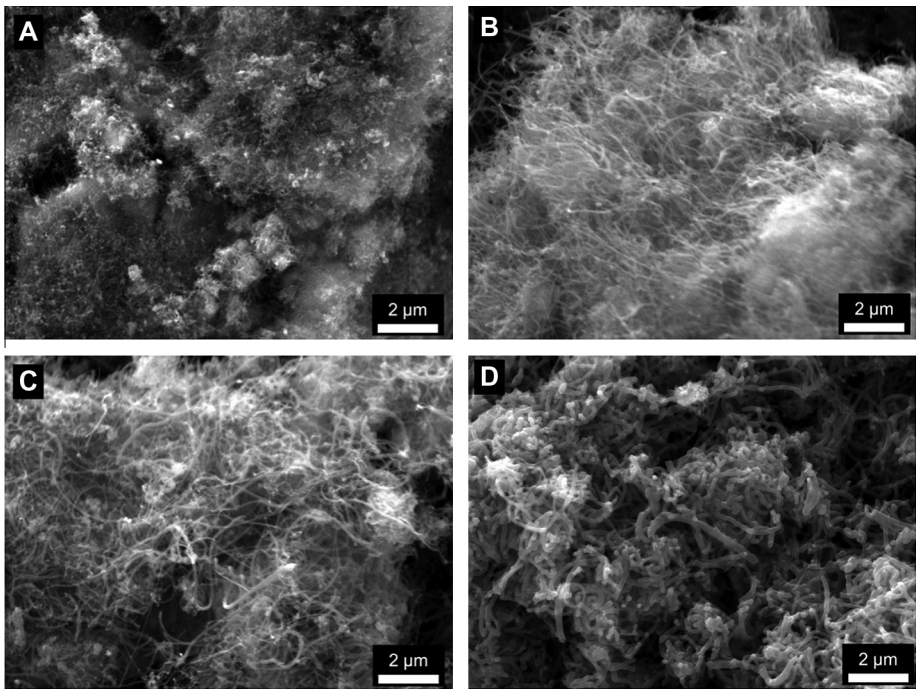

Fig. 3 – SEM micrographs of N-CNTs synthesized at (A) 550 °C, (B) 750 °C, (C) 850 °C, and (D) 950 °C.

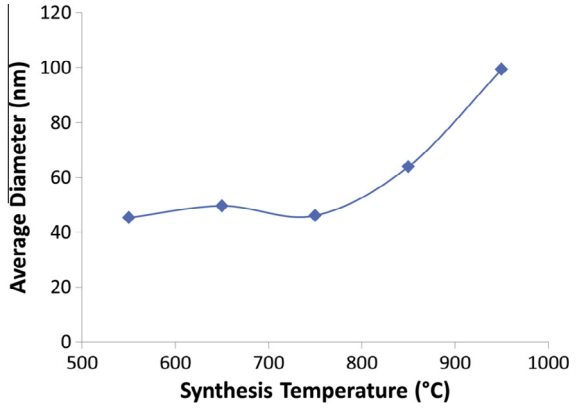

Fig. 4 – Distribution of the average diameter of N-CNTs as a function of synthesis temperature. (A color version of this figure can be viewed online.)

ported [9,29,42,46,55,56]. Terrones et al. proposed a mechanism for the growth of bamboo-like N-CNTs on a cobalt catalyst [55]. With this growth mechanism, they suggested that the during the growth of N-CNTs, graphitic layers form on the catalyst nanoparticles, creating a cone-shaped cup-like structure consisting of closely fitting nested graphene components with various strains inside the cup. These strains relax with a sudden sliding of the cup, and the next graphitic layers form on the catalyst underneath the first cap. This process continues until the formation of the complete N-CNT.

In another work, van Dommele et al. reported that this capping was directly linked to the nature of the catalyst for the growth of N-CNTs [46]. Based on their results, the use of iron as the catalyst for the growth of N-CNTs led to the formation of a bamboo-like structure; whereas the use of nickel and cobalt led to the formation of open channel N-CNTs.

Based on TEM images, very low amounts of amorphous carbon were found on the N-CNTs synthesized at temperatures lower than 950 °C. For N-CNTs synthesized at 950 °C, the structure of the carbon nanotubes appeared more disordered with less homogeneous diameter distribution. The TEM images also demonstrated a greater population density of amorphous carbon in the sample synthesized at 950 °C than at lower temperatures (shown by arrows in Fig. 5C and D).

The lengths of N-CNTs were measured for more than 70 nanotubes per sample using TEM images. The graph of the N-CNT length as a function of synthesis temperature in Fig. 6A demonstrates that the average N-CNT length increased when the synthesis temperature increased up to 750 °C. Higher temperatures increased the diameter of the N-CNTs, but no significant increase in length was observed.

The aspect ratios of N-CNTs were calculated and are shown as a function of synthesis temperature in Fig. 6B. The highest aspect ratio for the N-CNTs was obtained at a synthesis temperature of 750 °C. This temperature is high enough for the effective growth of N-CNTs, as the carbon and nitrogen precursors have enough energy to decompose and form N-CNTs, but is not high enough for the migration and sintering of the catalyst.

3.1.3. *Structural defects*

The incorporation of dopants, such as nitrogen, in CNTs has been shown to create defects, which can be tracked with Raman spectroscopy [57–59]. Raman spectra of CNTs have several characteristic bands that provide information on the extent of disordering and changes in the electronic structure as a result of nitrogen doping [60]. In Fig. 7 Raman spectra of undoped CNTs are compared to nitrogen-doped CNTs (N-CNTs) at a synthesis temperature of 650 °C. The spectra dis-

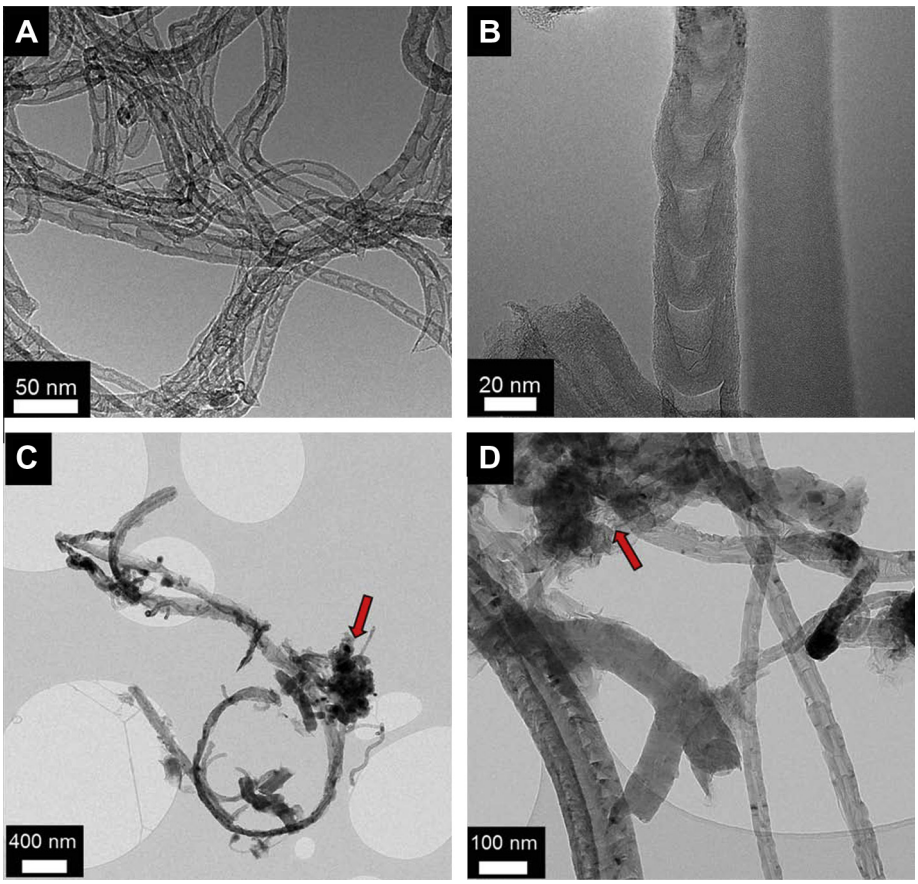

Fig. 5 – TEM micrographs of N-CNTs synthesized at (A and B) 650 °C and (C and D) 950 °C, showing the bamboo-like structure of N-CNTs. The samples synthesized at temperatures lower than 950 °C had less amorphous carbon. Disordered carbon materials were found in the N-CNTs synthesized at 950 °C (shown by arrows in C and D). (A color version of this figure can be viewed online.)

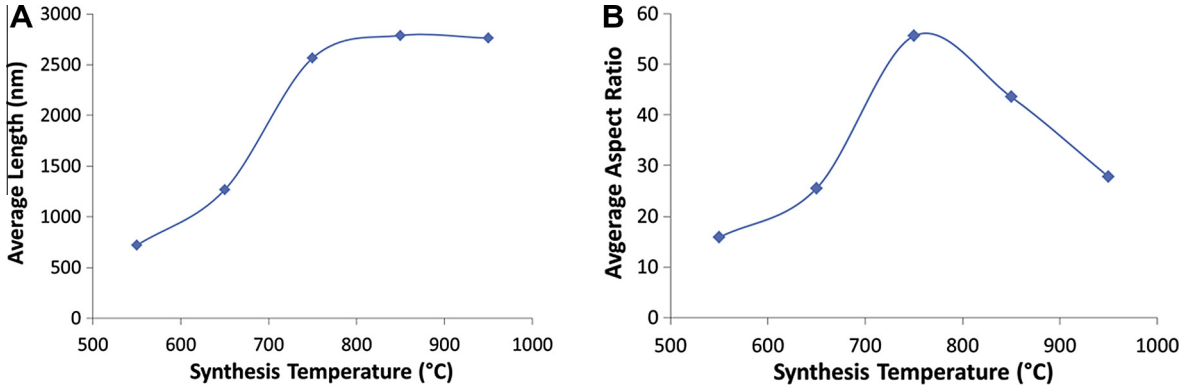

Fig. 6 – (A) The lengths of N-CNTs measured from TEM images, showing the increases in length by increasing the synthesis temperature to 750 °C. (B) The average aspect ratio (length/diameter) of N-CNTs as a function of synthesis temperature, showing the optimal temperature of 750 °C for higher length and smaller diameter N-CNTs. (A color version of this figure can be viewed online.)

play the expected bands found in graphitic materials and these are denoted as the G, D, and G′-bands. The G-band (~1600 cm^{-1}) results from C—C stretching in sp^2 carbon networks and is found in all Raman spectra of graphitic carbon. The D-band or also called the "disorder-band" (~1400 cm^{-1}) is a direct measure of disorder in the carbon network as this mode only becomes Raman active due to a loss of symmetry near crystalline edges [59]. The G′-band (~2700 cm^{-1}) is sensitive to changes in the electronic structure of the graphitic layers and can thus be utilized to evaluate the degree of doping in CNTs, as the integration of nitrogen in CNTs changes the electronic and catalytic properties of these CNTs [58,60,61].

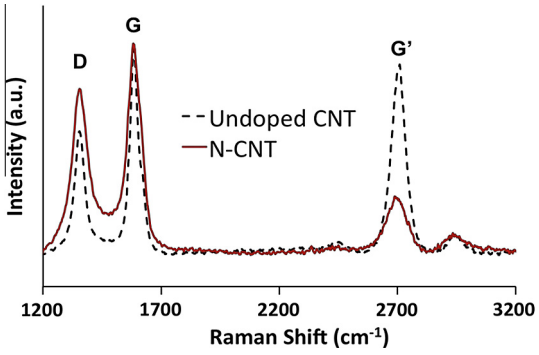

Fig. 7 – Raman spectra of both undoped and nitrogen-doped CNTs synthesized at 650 °C. (A color version of this figure can be viewed online.)

Moreover, the position and intensity of this band are highly dependent on the excitation laser frequency [60,62].

Although the individual bands provide ample information about the graphitic structure, the D-band over the G-band intensity ratio (I_D/I_G) is a numerical measure often used in conjunction with Raman analysis of CNTs. This ratio is a good estimator of the graphite crystalline length and thus a measure of disorder [59]. The intensity ratio of $I_{G'}/I_G$ is utilized for measurements involving changes in electronic properties of CNTs as a result of nitrogen doping [57].

The Raman spectra showed a clear increase in the I_D/I_G ratio for N-CNTs (0.82 ± 0.05) compared to undoped CNTs (0.66 ± 0.07), indicating more defects in the N-CNT structure. This phenomenon can be explained by the integration of nitrogen atoms in the carbon nanotube structure, which diminishes the ordering of the graphitic network. The various types of nitrogen incorporation in N-CNTs show an abundance of forms in which the hexagonal carbon rings can be disturbed. This disturbance in the graphene sheets, which can lead to the formation of pentagons, heptagons or replacement of nitrogen in the hexagonal carbon rings, results in changes in the electronic properties of the modified CNTs [63]. Such changes in the electronic structure can impart a metallic character to CNTs by providing electron donor states near the conduction band [64]. A direct comparison of the $I_{G'}/I_G$ ratio from undoped CNTs (0.93 ± 0.06) and N-CNTs (0.22 ± 0.04) in Fig. 7 indicates that nitrogen doping significantly lowers the $I_{G'}/I_G$ ratio.

The amount and type of nitrogen can be controlled by employing a range of synthesis temperatures, as discussed in Section 3.1.1. This effect of temperature on the density of defects in the N-CNT structure was investigated by Raman spectroscopy. The various Raman spectra of N-CNTs synthesized at different temperatures are shown in Fig. 8A. The D-band increased in intensity as the synthesis temperature was lowered.

Fig. 8B shows the I_D/I_G ratios for the N-CNTs synthesized at different temperatures. This ratio decreased with increasing synthesis temperature, indicating a higher degree of crystallinity in the N-CNT structure produced at higher temperatures. The I_D/I_G ratio for the N-CNT sample synthesized at 950 °C did not follow the expected trend; instead the ratio appears to have increased again, indicating more defects in its structure. This conclusion is supported by the TEM analysis for that specific sample, which showed structural diversity in the N-CNTs, exhibiting low to high crystallinity in the graphitic network, including regions containing amorphous carbon. The I_D/I_G ratio for this sample synthesized at 950 °C also contained a very large error, which can be explained by the structural diversity of the sample.

The results obtained from the Raman analysis are in a good agreement with the XPS derived results, showing a decrease in the nitrogen content as the synthesis temperature increased from 550 to 850 °C, followed by a reversal at 950 °C, leading to an increase in the percentage of nitrogen. This I_D/I_G ratio behavior as a function of nitrogen doping is well documented in the literature, further supporting our findings [57–59].

The other aspect in the Raman spectra of N-CNTs synthesized at different temperatures is the G′-band, which was explored in the form of the $I_{G'}/I_G$ ratio for the temperature range from 550 to 950 °C and is shown in Fig. 8C. The $I_{G'}/I_G$ ratio increased significantly, going from 0.04 ± 0.02 for the N-CNT sample at 550 °C to 0.60 ± 0.1 for the sample at 750 °C. The ratio for the samples at 750, 850 and 950 °C remained fairly constant, ranging from 0.5 ± 0.1 to 0.60 ± 0.1.

The $I_{G'}/I_G$ ratio appeared to have two distinct regions, which was also observed by Sharifi et al. [57]. The ratio initially increased as the nitrogen content in the CNTs decreased to approximately 2% (corresponding to a synthesis temperature of 750 °C), at which point the trend leveled off or slightly reversed. Sharifi et al. observed this turning point at approximately 5%, which differs from the results presented in this study. A report by Bulusheva et al. [58] showed an opposite trend, in which the $I_{G'}/I_G$ ratio increased as the nitrogen concentration was raised from 0% to 1%. We cannot account for this behavior, as the nitrogen content investigated in the present work was greater than 2%.

3.1.4. *Thermal stability*

The thermal stability of N-CNTs was tested using TGA, and the results are shown in Fig. 9. As observable in Fig. 9, the oxidation temperature increased with increasing synthesis temperature up to 950 °C. Increasing the synthesis temperature led to a higher crystallinity of the graphitic structure of N-CNTs, with a lower concentration of defects and nitrogen content in the N-CNT structure. These defects can initiate oxidation at lower temperatures. The oxidation temperature of the N-CNTs synthesized at 850 °C was more than 100 °C higher than the N-CNTs synthesized at 550 °C, demonstrating the higher stability of the N-CNT structure synthesized at higher temperatures.

The N-CNTs synthesized at 950 °C did not follow this trend and were observed to have a lower thermal stability than the N-CNTs synthesized at 750 and 850 °C. This may be related to the presence of other types of carbon allotropes that have lower thermal stability, such as amorphous carbon, which lowers the overall oxidation temperature of the sample synthesized at 950 °C.

The TGA tests revealed that some material remains even after exposure to high oxidation temperatures. This residue is mostly comprised of the catalyst used for the growth of N-CNTs. The overall percentage of impurities that were left

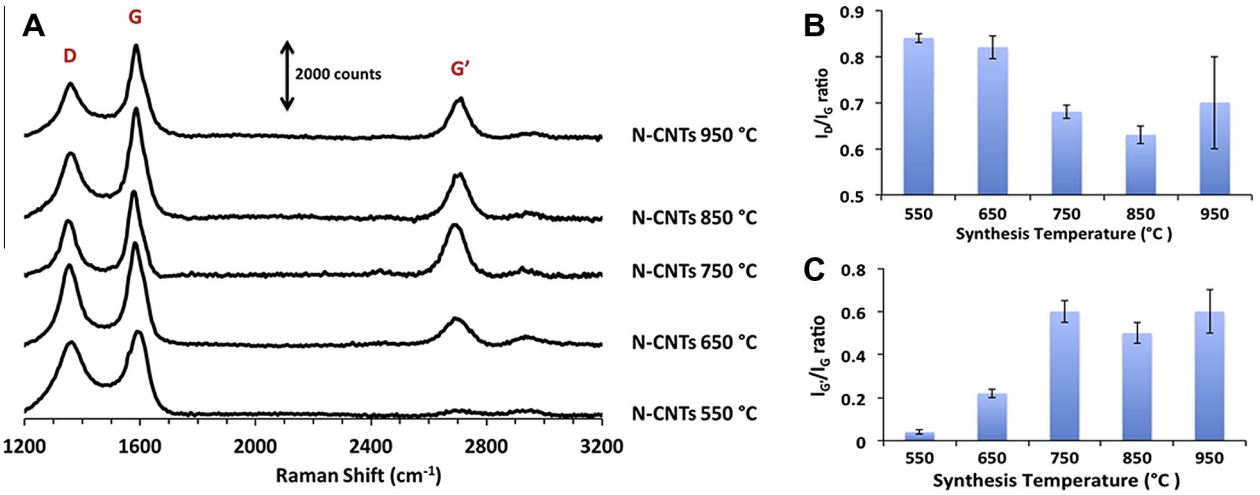

Fig. 8 – (A) Raman spectra of N-CNTs synthesized at 550, 650, 750, 850, and 950 °C. (B) The ratio of the D- and G-band intensities versus synthesis temperature. (C) The ratio of the G′- and G-band intensities versus synthesis temperature. Error bars are derived from the standard deviation of $n = 3$ measurements. (A color version of this figure can be viewed online.)

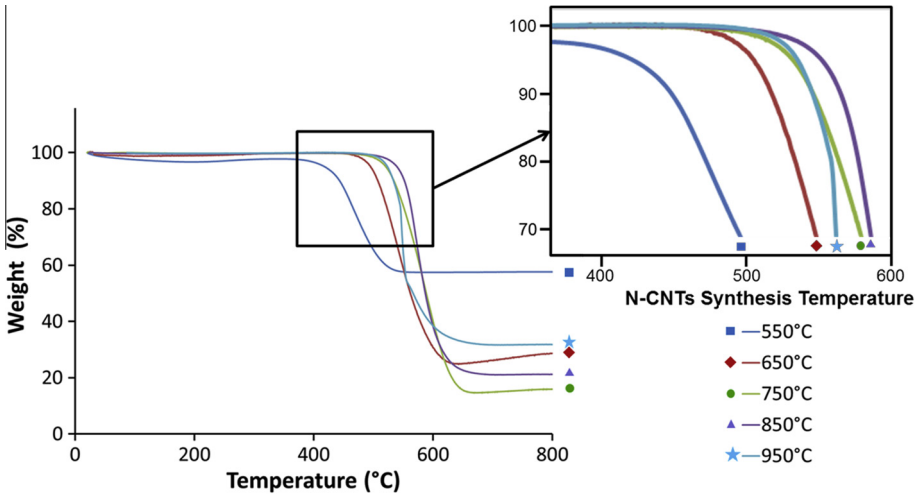

Fig. 9 – TGA thermograms of N-CNTs synthesized at different temperatures. (A color version of this figure can be viewed online.)

behind after burning depended on the synthesis conditions and yields, which will be discussed in more detail later.

The thermal stability of N-CNTs was also compared to undoped CNTs using TGA. The TGA results displayed in Fig. 10 show a higher thermal stability for the undoped CNTs compared to N-CNTs synthesized at similar temperatures. This higher thermal stability of undoped CNTs may be related to the lower number of defects in their structure, making them more resistant to oxidation.

3.2. *The effect of synthesis temperature and synthesis time on the yield of N-CNTs*

In the condition with low N-CNT yield, most of the material will be lost after purification. This may lead to some difficulties for their future applications. In this work, the yield of N-CNTs is reported as the product mass and has been plotted as a function of different synthesis temperatures and synthesis times. These results give us good idea as to which synthesis conditions are more favorable for providing high yield of the product.

The synthesis temperature had an obvious influence on the N-CNTs yield. The product mass increased with increasing synthesis temperature from 550 to 750 °C (Fig. 11), which may be attributed to the fact that there is more energy at higher temperatures for the decomposition of the carbon and nitrogen precursors and formation of N-CNTs. However at temperatures higher than 750 °C, a lower product mass was obtained, which may be related to the formation of types of carbon allotropes other than carbon nanotubes such as amorphous carbon. These allotropes of carbon can cover and deactivate the catalyst, resulting in a lower yield. The deactivation of the catalyst can also be related to the formation of stable metal carbides that will not play the role of catalyst [65].

The yield can also be controlled by changing the synthesis time. The product mass increased with increasing synthesis

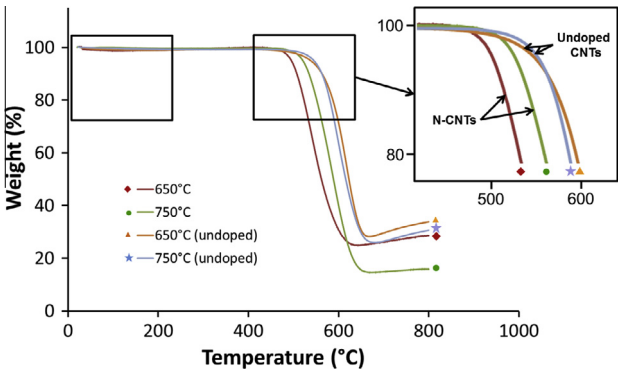

Fig. 10 – TGA thermograms of N-CNTs and undoped CNTs synthesized at 650 and 750 °C. (A color version of this figure can be viewed online.)

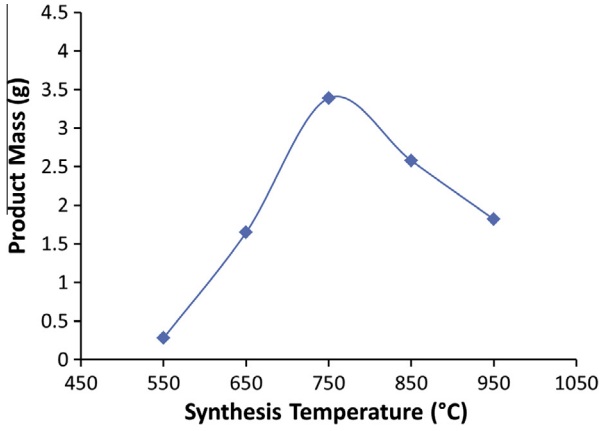

Fig. 11 – Product mass as a function of synthesis temperature, showing the highest N-CNT mass for the sample synthesized at 750 °C. (A color version of this figure can be viewed online.)

time, as more carbon source was provided for N-CNT production (Fig. 12A). The increasing trend of the yield at 750 °C was linear up to about 2 h, with the product mass almost doubling when the synthesis time was increased from 1 to 2 h. A synthesis time of 3 h increased the product mass, but not significantly; and, the slope of the curve decreased with increasing time. This can be related to the lower accessibility of the catalyst to the reactants, due to the carbon product that covers the catalyst as they grow over the catalyst.

The average length of the N-CNTs obtained from TEM images showed increased N-CNT length with increasing synthesis time (Fig. 12B). This increase is related to the higher amount of carbon precursor entering the reactor at longer synthesis times, which leads to formation of longer N-CNTs on the active catalysts. The maximum average N-CNT length obtained was around 2.5 μm. Although the length of N-CNTs increased by increasing the synthesis time, this trend leveled off after 2 h of synthesis. This may be related to lower accessibility of the catalyst as the product covers it over time.

4. Conclusions

Nitrogen-doped carbon nanotubes (N-CNTs) were synthesized via a chemical vapor deposition method, using ammonia as the source of nitrogen and ethane as the source of carbon. The effects of the synthesis temperature on different properties of N-CNTs were investigated. It was determined that the nitrogen content in the N-CNTs decreased with increasing synthesis temperature in the range between 550 and 850 °C. The synthesis temperature not only affected the nitrogen content of the N-CNTs, but also varied the type of nitrogen incorporation. The average diameter and length of N-CNTs were increased with increasing synthesis temperature. The highest aspect ratio of the N-CNTs was obtained for N-CNTs synthesized at 750 °C. TEM results revealed a mainly bamboo-like structure for N-CNTs.

Raman spectra showed higher crystallinity for N-CNTs synthesized at higher temperatures in the range of 550–850 °C. The Raman test also showed that there was a higher number of defects in the N-CNT structure than in the structure of undoped CNTs. In the same temperature range, the thermal stability of the N-CNTs increased with increasing synthesis temperature. However the crystallinity and thermal stability of the N-CNTs synthesized at 950 °C were lower than for N-CNTs synthesized

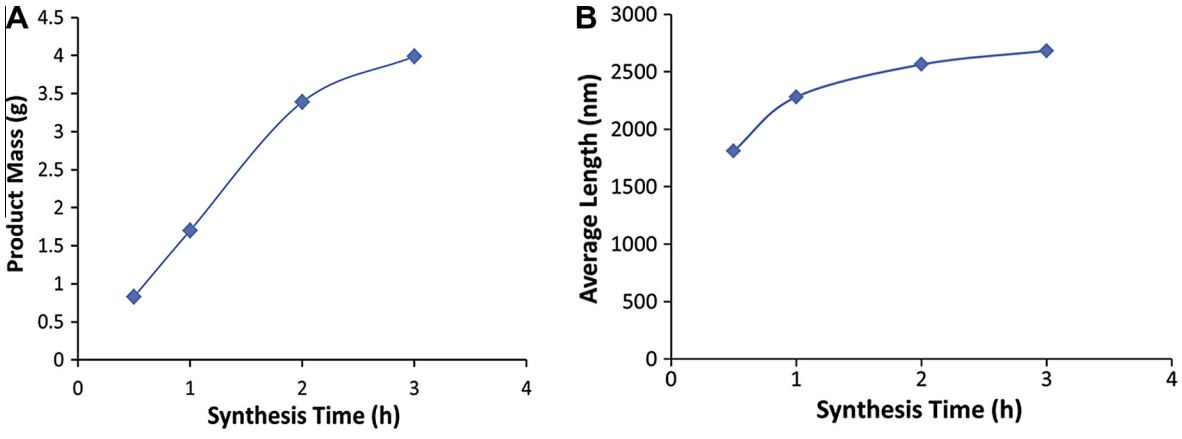

Fig. 12 – (A) Product mass as a function of the synthesis time. (B) Average length of N-CNTs as a function of the synthesis time. N-CNTs were synthesized at 750 °C. (A color version of this figure can be viewed online.)

at 850 °C. This can be attributed to the presence of amorphous carbon, which decreases the crystallinity and burns at a lower temperature than the carbon nanotubes.

The yield was also influenced by synthesis parameters. The synthesis temperature affected the yield, and the highest N-CNT mass was obtained at 750 °C. Increase in synthesis time also increased the product mass and the average length of N-CNTs. These results will provide insight towards controlling some of the most important properties of nitrogen-doped carbon nanotubes, such as concentration and type of nitrogen incorporations, structural defects, thermal stability, aspect ratio and yield, by changing the synthesis temperature.

Acknowledgements

The authors acknowledge support for this project from Natural Sciences and Engineering Research Council of Canada (NSERC). We would like to thank Drs. Hebert Molero, Tobias Fürstenhaupt, Mark McDermott and Michael Schoel for their help in X-ray photoelectron spectroscopy (XPS), transmission electron microscopy (TEM), Raman spectroscopy and scanning electron microcopy (SEM) analyses, respectively. The XPS analyses were done in the Catalysis Surface Science Laboratory at the University of Calgary. TEM and SEM were done by the Microscopy and Imaging Facility (MIF) of the University of Calgary.

REFERENCES

[1] Iijima S. Helical microtubules of graphitic carbon. Nature 1991;354(6348):56–8.
[2] Golberg D, Bando Y, Han W, Kurashima K, Sato T. Single-walled B-doped carbon, B/N-doped carbon and BN nanotubes synthesized from single-walled carbon nanotubes through a substitution reaction. Chem Phys Lett 1999;308(3–4):337–42.
[3] Redlich P, Loeffler J, Ajayan PM, Bill J, Aldinger F, Rühle M. B–C–N nanotubes and boron doping of carbon nanotubes. Chem Phys Lett 1996;260(3–4):465–70.
[4] Peng S, Cho K. Ab initio study of doped carbon nanotube sensors. Nano Lett 2003;3(4):513–7.
[5] Li YT, Chen TC. Effect of B/N co-doping on the stability and electronic structure of single-walled carbon nanotubes by first-principles theory. Nanotechnology 2009;20(37).
[6] Gong K, Du F, Xia Z, Durstock M, Dai L. Nitrogen-doped carbon nanotube arrays with high electrocatalytic activity for oxygen reduction. Science 2009;323(5915):760–4.
[7] Terrones M, Ajayan PM, Banhart F, Blase X, Carroll DL, Charlier JC, et al. N-doping and coalescence of carbon nanotubes: synthesis and electronic properties. Appl Phys A Mater Sci Process 2002;74(3):355–61.
[8] Ewels CP, Glerup M. Nitrogen doping in carbon nanotubes. J Nanosci Nanotechnol 2005;5(9):1345–63.
[9] Chizari K, Janowska I, Houllé M, Florea I, Ersen O, Romero T, et al. Tuning of nitrogen-doped carbon nanotubes as catalyst support for liquid-phase reaction. Appl Catal A Gen 2010;380(1–2):72–80.
[10] Sharma RB, Late DJ, Joag DS, Govindaraj A, Rao CNR. Field emission properties of boron and nitrogen doped carbon nanotubes. Chem Phys Lett 2006;428(1–3):102–8.
[11] Ghosh K, Kumar M, Maruyama T, Ando Y. Controllable growth of highly N-doped carbon nanotubes from imidazole: a structural, spectroscopic and field emission study. J Mater Chem 2010;20(20):4128–34.
[12] Baierle RJ, Piquini P, Schmidt TM, Fazzio A. Hydrogen adsorption on carbon-doped boron nitride nanotube. J Phys Chem B 2006;110(42):21184–8.
[13] Yu SS, Wen QB, Zheng WT, Jiang Q. Effects of doping nitrogen atoms on the structure and electronic properties of zigzag single-walled carbon nanotubes through first-principles calculations. Nanotechnology 2007;18(16).
[14] Giambastiani G, Cicchi S, Giannasi A, Luconi L, Rossin A, Mercuri F, et al. Functionalization of multiwalled carbon nanotubes with cyclic nitrones for materials and composites: addressing the role of CNT sidewall defects. Chem Mater 2011;23(7):1923–38.
[15] Van Dommele S, De Jong KP, Bitter JH. Nitrogen-containing carbon nanotubes as solid base catalysts. Chem Commun 2006;46:4859–61.
[16] Chizari K, Deneuve A, Ersen O, Florea I, Liu Y, Edouard D, et al. Nitrogen-doped carbon nanotubes as a highly active metal-free catalyst for selective oxidation. ChemSusChem 2012;5(1):102–8.
[17] Jin C, Nagaiah TC, Xia W, Spliethoff B, Wang S, Bron M, et al. Metal-free and electrocatalytically active nitrogen-doped carbon nanotubes synthesized by coating with polyaniline. Nanoscale 2010;2(6):981–7.
[18] Morozan A, Jégou P, Pinault M, Campidelli S, Jousselme B, Palacin S. Metal-free nitrogen-containing carbon nanotubes prepared from triazole and tetrazole derivatives show high electrocatalytic activity towards the oxygen reduction reaction in alkaline media. ChemSusChem 2012;5(4):647–51.
[19] Li Y, Zhou W, Wang H, Xie L, Liang Y, Wei F, et al. An oxygen reduction electrocatalyst based on carbon nanotube–graphene complexes. Nat Nanotechnol 2012;7(6):394–400.
[20] Tuci G, Zafferoni C, D'Ambrosio P, Caporali S, Ceppatelli M, Rossin A, et al. Tailoring carbon nanotube N-dopants while designing metal-free electrocatalysts for the oxygen reduction reaction in alkaline medium. ACS Catal 2013;3(9):2108–11.
[21] Geng D, Chen Y, Chen Y, Li Y, Li R, Sun X, et al. High oxygen-reduction activity and durability of nitrogen-doped graphene. Energy Environ Sci 2011;4(3):760–4.
[22] Zhu J, Holmen A, Chen D. Carbon nanomaterials in catalysis: proton affinity, chemical and electronic properties, and their catalytic consequences. ChemCatChem 2013;5(2):378–401.
[23] Ghosh K, Kumar M, Maruyama T, Ando Y. Tailoring the field emission property of nitrogen-doped carbon nanotubes by controlling the graphitic/pyridinic substitution. Carbon 2010;48(1):191–200.
[24] Wang EG. New development in covalently bonded carbon nitride and related materials. Adv Mater (Weinheim, Ger) 1999;11(13):1129–33.
[25] Lee CJ, Lyu SC, Kim HW, Lee JH, Cho KI. Synthesis of bamboo-shaped carbon–nitrogen nanotubes using C_2H_2–NH_3–$Fe(CO)_5$ system. Chem Phys Lett 2002;359(1–2):115–20.
[26] Sen R, Satishkumar BC, Govindaraj A, Harikumar KR, Renganathan MK, Rao CNR. Nitrogen-containing carbon nanotubes. J Mater Chem 1997;7(12):2335–7.
[27] Glerup M, Castignolles M, Holzinger M, Hug G, Loiseau A, Bernier P. Synthesis of highly nitrogen-doped multi-walled carbon nanotubes. Chem Commun 2003;9(20):2542–3.
[28] Terrones M, Terrones H, Grobert N, Hsu WK, Zhu YQ, Hare JP, et al. Efficient route to large arrays of CNx nanofibers by pyrolysis of ferrocene/melamine mixtures. Appl Phys Lett 1999;75(25):3932–4.
[29] Trasobares S, Stéphan O, Colliex C, Hsu WK, Kroto HW, Walton DRM. Compartmentalized CNx nanotubes: chemistry, morphology, and growth. J Chem Phys 2002;116(20):8966–72.

[30] Terrones M, Redlich P, Grobert N, Trasobares S, Hsu WK, Terrones H, et al. Carbon nitride nanocomposites: formation of aligned CxNy Nanofibers. Adv Mater (Weinheim, Ger) 1999;11(8):655–8.
[31] Tang C, Bando Y, Golberg D, Xu F. Structure and nitrogen incorporation of carbon nanotubes synthesized by catalytic pyrolysis of dimethylformamide. Carbon 2004;42(12–13):2625–33.
[32] Terrones M, Grobert N, Olivares J, Zhang JP, Terrones H, Kordatos K, et al. Controlled production of aligned-nanotube bundles. Nature 1997;388(6637):52–5.
[33] Suenaga K, Yudasaka M, Colliex C, Iijima S. Radially modulated nitrogen distribution in CNx nanotubular structures prepared by CVD using Ni phthalocyanine. Chem Phys Lett 2000;316(5–6):365–72.
[34] Yudasaka M, Kikuchi R, Ohki Y, Yoshimura S. Nitrogen-containing carbon nanotube growth from Ni phthalocyanine by chemical vapor deposition. Carbon 1997;35(2):195–201.
[35] Wang X, Hu W, Liu Y, Long C, Xu Y, Zhou S, et al. Bamboo-like carbon nanotubes produced by pyrolysis of iron(II) phthalocyanine. Carbon 2001;39(10):1533–6.
[36] Terrones M, Kamalakaran R, Seeger T, Ruhle M. Novel nanoscale gas containers: encapsulation of N_2 in CN(x) nanotubes. Chem Commun 2000;23:2335–6.
[37] Lee YT, Kim NS, Bae SY, Park J, Yu SC, Ryu H, et al. Growth of vertically aligned nitrogen-doped carbon nanotubes: control of the nitrogen content over the temperature range 900–1100 °C. J Phys Chem B 2003;107(47):12958–63.
[38] Liu J, Webster S, Carroll DL. Temperature and flow rate of NH_3 effects on nitrogen content and doping environments of carbon nanotubes grown by injection CVD method. J Phys Chem B 2005;109(33):15769–74.
[39] Min YS, Bae EJ, Asanov IP, Kim UJ, Park W. Growth and characterization of nitrogen-doped single-walled carbon nanotubes by water-plasma chemical vapour deposition. Nanotechnology 2007;18(28).
[40] Tao XY, Zhang XB, Sun FY, Cheng JP, Liu F, Luo ZQ. Large-scale CVD synthesis of nitrogen-doped multi-walled carbon nanotubes with controllable nitrogen content on a CoxMg1–xMoO4 catalyst. Diamond Relat Mater 2007;16(3):425–30.
[41] Jang JW, Lee CE, Lyu SC, Lee TJ, Lee CJ. Structural study of nitrogen-doping effects in bamboo-shaped multiwalled carbon nanotubes. Appl Phys Lett 2004;84(15):2877–9.
[42] Amadou J, Chizari K, Houllé M, Janowska I, Ersen O, Bégin D, et al. N-doped carbon nanotubes for liquid-phase C=C bond hydrogenation. Catal Today 2008;138(1–2):62–8.
[43] Sen R, Satishkumar BC, Govindaraj A, Harikumar KR, Raina G, Zhang JP, et al. B–C–N, C–N and B–N nanotubes produced by the pyrolysis of precursor molecules over Co catalysts. Chem Phys Lett 1998;287(5–6):671–6.
[44] Che R, Peng LM, Chen Q, Duan XF, Gu ZN. Fe_2O_3 particles encapsulated inside aligned CN_x nanotubes. Appl Phys Lett 2003;82(19):3319–21.
[45] Zhang Y, Pan L, Wen B, Xiaoyang S, Liu C, Li T. Influence of growth temperature on the structure, composition and bonding character of nitrogen-doped multiwalled carbon nanotubes. J Mater Res 2011;26(3):443–8.
[46] van Dommele S, Romero-Izquirdo A, Brydson R, de Jong KP, Bitter JH. Tuning nitrogen functionalities in catalytically grown nitrogen-containing carbon nanotubes. Carbon 2008;46(1):138–48.
[47] Wiggins-Camacho JD, Stevenson KJ. Effect of nitrogen concentration on capacitance, density of states, electronic conductivity, and morphology of N-doped carbon nanotube electrodes. J Phys Chem C 2009;113(44):19082–90.
[48] Wei J, Hu H, Zeng H, Zhou Z, Yang W, Peng P. Effects of nitrogen substitutional doping on the electronic transport of carbon nanotube. Phys E Low Dimensional Syst Nanostruct 2008;40(3):462–6.
[49] Biniak S, Szymański G, Siedlewski J, Światkoski A. The characterization of activated carbons with oxygen and nitrogen surface groups. Carbon 1997;35(12):1799–810.
[50] Choi HC, Bae SY, Park J, Seo K, Kim C, Kim B, et al. Experimental and theoretical studies on the structure of N-doped carbon nanotubes: possibility of intercalated molecular N_2. Appl Phys Lett 2004;85(23):5742–4.
[51] Choi HC, Park J, Kim B. Distribution and structure of N atoms in multiwalled carbon nanotubes using variable-energy X-ray photoelectron spectroscopy. J Phys Chem B 2005;109(10):4333–40.
[52] Lahaye J, Nansé G, Bagreev A, Strelko V. Porous structure and surface chemistry of nitrogen containing carbons from polymers. Carbon 1999;37(4):585–90.
[53] Öncel C, Yürüm Y. Carbon nanotube synthesis via the catalytic CVD method: a review on the effect of reaction parameters. Fullerenes Nanotubes Carbon Nanostruct 2006;14(1):17–37.
[54] Kaatz FH, Siegal MP, Overmyer DL, Provencio PP, Jackson JL. Diameter control and emission properties of carbon nanotubes grown using chemical vapor deposition. Mater Sci Eng C 2003;23(1–2):141–4.
[55] Terrones M, Benito AM, Manteca-Diego C, Hsu WK, Osman OI, Hare JP, et al. Pyrolytically grown BxCyNz nanomaterials: nanofibres and nanotubes. Chem Phys Lett 1996;257(5–6):576–82.
[56] Zhong D, Liu S, Zhang G, Wang EG. Large-scale well aligned carbon nitride nanotube films low temperature growth and electron field emission. J Appl Phys 2001;89(11 I):5939–43.
[57] Sharifi T, Nitze F, Barzegar HR, Tai CW, Mazurkiewicz M, Malolepszy A, et al. Nitrogen doped multi walled carbon nanotubes produced by CVD-correlating XPS and Raman spectroscopy for the study of nitrogen inclusion. Carbon 2012;50(10):3535–41.
[58] Bulusheva LG, Okotrub AV, Kinloch IA, Asanov IP, Kurenya AG, Kudashov AG, et al. Effect of nitrogen doping on Raman spectra of multi-walled carbon nanotubes. Phys Status Solidi B Basic Res 2008;245(10):1971–4.
[59] Maldonado S, Morin S, Stevenson KJ. Structure, composition, and chemical reactivity of carbon nanotubes by selective nitrogen doping. Carbon 2006;44(8):1429–37.
[60] Dresselhaus MS, Jorio A, Hofmann M, Dresselhaus G, Saito R. Perspectives on carbon nanotubes and graphene Raman spectroscopy. Nano Lett 2010;10(3):751–8.
[61] MacIel IO, Anderson N, Pimenta MA, Hartschuh A, Qian H, Terrones M, et al. Electron and phonon renormalization near charged defects in carbon nanotubes. Nat Mater 2008;7(11):878–83.
[62] Wang Y, Alsmeyer DC, McCreery RL. Raman spectroscopy of carbon materials: structural basis of observed spectra. Chem Mater 1990;2(5):557–63.
[63] Charlier JC. Defects in carbon nanotubes. Acc Chem Res 2002;35(12):1063–9.
[64] Czerw R, Terrones M, Charlier JC, Blase X, Foley B, Kamalakaran R, et al. Identification of electron donor states in N-doped carbon nanotubes. Nano Lett 2001;1(9):457–60.
[65] Yadav RM, Dobal PS, Shripathi T, Katiyar RS, Srivastava ON. Effect of growth temperature on bamboo-shaped carbon–nitrogen (C–N) nanotubes synthesized using ferrocene acetonitrile precursor. Nanoscale Res Lett 2009;4(3):197–203.